Available online at www.sciencedirect.com
SCIENCE DIRECT®
Journal of the European Ceramic Society 25 (2005) 529–534
www.elsevier.com/locate/jeurceramsoc

Nano- versus macro-hardness of liquid phase sintered SiC

M. Balog [a,*], P. Šajgalík [a], M. Hnatko [a], Z. Lenčéš [a], F. Monteverde [b], J. Kečkéš [c], J.-L. Huang [d]

[a] *Institute of Inorganic Chemistry, Slovak Academy of Sciences, Bratislava, Slovakia*
[b] *CNR-ISTEC, Research Institute for Ceramics Technology, Faenza, Italy*
[c] *Erich Schmid Institute for Materials Research, Austrian Academy of Sciences, Leoben, Austria*
[d] *Department of Materials Science and Engineering, National Cheng Kung University, Tainan, Taiwan, Republic of China*

Received 25 November 2003; received in revised form 21 January 2004; accepted 28 January 2004
Available online 4 June 2004

Abstract

Silicon carbide polycrystalline materials were prepared by liquid phase sintering. Different rare-earth oxides (Y_2O_3, Yb_2O_3, Sm_2O_3) and AlN were used as sintering additives. The final microstructure consists of core–rim structure owing to the incorporation of AlN into the rim of SiC grains by solid solution. Nano- versus macro-hardness of polycrystalline SiC materials were investigated in more details. The nano-hardness of SiC grains was in the range of 32–34 GPa and it depends on the chemical compositions of grains. The harness followed the core–rim chemistry of grains, showing lower values for the rim consisting of SiC–AlN solid solution. The comparison of nano- and macro-hardness showed that nano-hardness is significantly higher, generally by 5–7 GPa. The macro-hardness of tested samples had a larger scatter due to the influence of several factors: hardness of grains (nano-hardness), indentation size effect (ISE), microstructure, porosity, and grain boundary phase. The influence of grain boundary phase on macro-hardness is also discussed.

Keywords: SiC; Hardness; Grain growth; Nano-hardness

1. Introduction

Silicon carbide-based polycrystalline ceramics have been studied as potentially important structural material due to their excellent resistance to oxidation and corrosion, high temperature strength, thermal shock resistance, high wear resistance, and good thermal conductivity.

Silicon carbide itself is a highly covalent bonded compound. Therefore, it is difficult to densify the SiC-based materials without sintering additives. SiC can be sintered either by solid state sintering or liquid phase sintering with the aid of metal oxides, such as Al_2O_3 and Y_2O_3, which create liquid phase at temperatures 1850–2000 °C.[1–7] Several authors studied the influence of different rare-earth oxides on liquid phase sintering of SiC.[8,9] It was shown that rare-earth oxides might be as effective as Y_2O_3 in densification of SiC. Although, the chemical and physical properties of rare-earth oxides are similar, the difference in cationic field strength of individual rare-earth might result in different grain boundary phase properties and microstructure.[10,11] The microstructural development of liquid phase sintered SiC (LPS SiC) is controlled by solution-reprecipitation mechanism. LPS SiC exhibits microstructure consisting from SiC grains with core–rim structure. Generally, the core has a different chemistry compared with the rim, and therefore also different physical properties can be expected.[12,13]

In this work the nano-hardness of LPS SiC with core–rim structure has been investigated, and the correlation between nano and macro-hardness are discussed. The nano and macro-hardness is also related to the different rare-earth sintering additives. General affect of grain boundary phase on macro-hardness is discussed in more details.

2. Experimental

β-SiC powder (HSC-059, Superior Graphite, USA) was mixed with rare-earth oxides Y_2O_3 (H.C. Starck, Germany), Yb_2O_3 (H.C. Starck, Germany), Sm_2O_3 (Russia), and AlN (H.C. Starck, Germany). The chemical compositions of the studied samples are listed in Table 1. The amount of the sintering additives was 13 wt.% in total. The molar ratio of particular oxides was kept constant for all compositions 1:1.

* Corresponding author.
E-mail address: uachbalo@savba.sk (M. Balog).

0955-2219/$ – see front matter © 2004 Elsevier Ltd. All rights reserved.
doi:10.1016/j.jeurceramsoc.2004.01.026

Table 1
Chemical composition of samples (without impurities)

Sample	Composition (wt.%)					
	SiC	Seeds	AlN	Y_2O_3	Yb_2O_3	Sm_2O_3
SCα-Y	85	2 (α)	3	10	–	–
SCα-YYb	85	2 (α)	3	4.60	5.40	–
SCα-YSm	85	2 (α)	3	3.93	–	6.07
SCα-YbSm	85	2 (α)	3	–	5.30	4.70
SCβ-Y	85	2 (β)	3	10	–	–
SCβ-YYb	85	2 (β)	3	4.60	5.40	–
SCβ-YSm	85	2 (β)	3	3.93	–	6.07
SCβ-YbSm	85	2 (β)	3	–	5.30	4.70

Moreover, 2 wt.% of α-SiC (C-Axis Technology, Canada) or β-SiC (Tokai Carbon, Japan) seeds were added to the starting powder mixture. The powder mixtures were ball milled in isopropanol with SiC balls for 24 h. The homogenized suspension was dried, subsequently sieved through 75 μm sieve screen in order to avoid hard agglomerates. Axially pressed samples, 12 mm in diameter and 10 mm high, were embedded in BN and located into graphite die. Afterwards the samples were hot pressed at 1850 °C for 1 h under mechanical pressure of 30 MPa in Ar + N_2 atmosphere. Hot pressed samples were subsequently annealed for 10 h at 1850 °C in Ar + N_2 atmosphere. The densities of samples were measured by Archimedes method in mercury. The theoretical densities were calculated according to the rule of mixtures. The hot-pressed materials were cut, polished, and plasma etched with CF_4 + 10% O_2 gas mixture for the microstructure analysis. The microstructures were observed by scanning electron microscopy (SEM). The chemical composition of crystalline grains was examined by EDX. Vickers macro-hardness was measured using LECO Hardness Tester, Model LV-100AT by indentation method with a load of 9.8 N. Nano-hardness of SiC grains was investigated by atomic force microscopy (AFM, HYSITRON nano-hardness tester) using the Berkovich indenter. The nano-hardness was obtained by depth-sensing method. The preliminary nano-hardness measurements exhibited "indentation size effect" for all compositions. Systematic study of the applied load versus nano-hardness showed an optimal loading about 3.5 mN for the LPS SiC. At this load the surface layer had no influence on measured hardness values and crack formation was not observed. Each sample was indented more than 70 times, while the imprints near the microstructural defects (pores, removed grains, etc.) were excluded from the evaluation.

3. Results and discussion

All samples were sintered to near theoretical densities. The microstructure of hot-pressed samples consists of equiaxed grains (Fig. 1). Generally, all hot pressed samples doped with β-SiC seeds have bigger grains compared with samples doped with α-SiC seeds. Grain growth was observed after 10 h annealing for all compositions, however, the growth rate was dependent on the chemical composition of additives. More pronounced grain growth was observed for the samples doped with β-SiC seeds compared to the samples doped with α-SiC seeds in all studied cases. Characteristic microstructures of samples annealed for 10 h are shown in Fig. 2.

The Vickers macro-hardness (9.81 N load) of samples is shown in Fig. 3. Samples doped with α-SiC seeds are harder compared with β-SiC doped ones for identical chemical composition of additives. The hardness of hot pressed samples (HP) increased after annealing (AN10) for all samples, most probably due to evaporation of the oxide grain boundary phases during annealing (grain boundary thinning).[11,12]

3.1. Nano-hardness

Characteristic AFM scan image of sample before and after indentation is shown in Fig. 4. The dark triangles are the indentation imprints. The nano-hardness of hot-pressed (HP) and 10 h annealed samples (AN10) are plotted in Fig. 5, except sample SCα-YYb. Taking into account also the error bars, it can be concluded that the nano-hardness is almost the same for all compositions. A small deviation is visible only for the hot-pressed sample SCα-Y. It should be pointed out

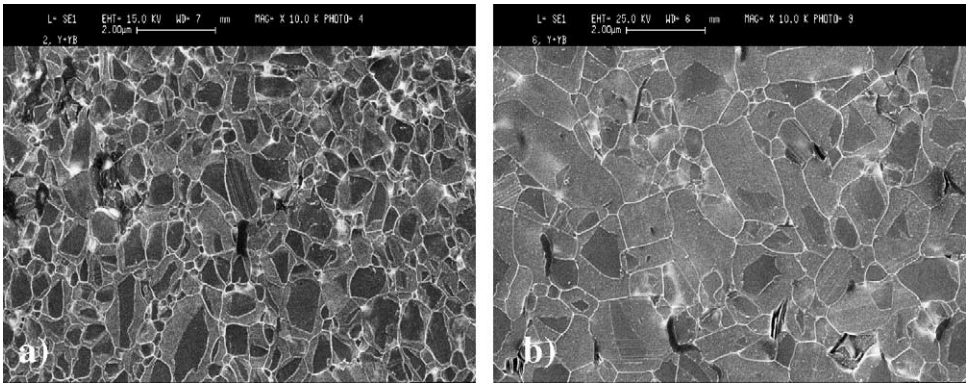

Fig. 1. Characteristic microstructure of hot pressed samples (1850 °C/1h): (a) SCα-YbSm and (b) SCβ-YbSm.

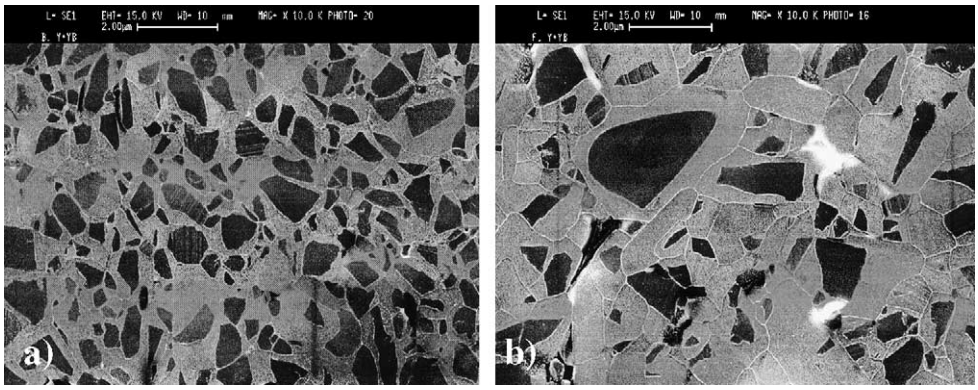

Fig. 2. Characteristic microstructure of annealed samples (1850 °C/10 h): (a) SCα-YYb and (b) SCβ-YYb.

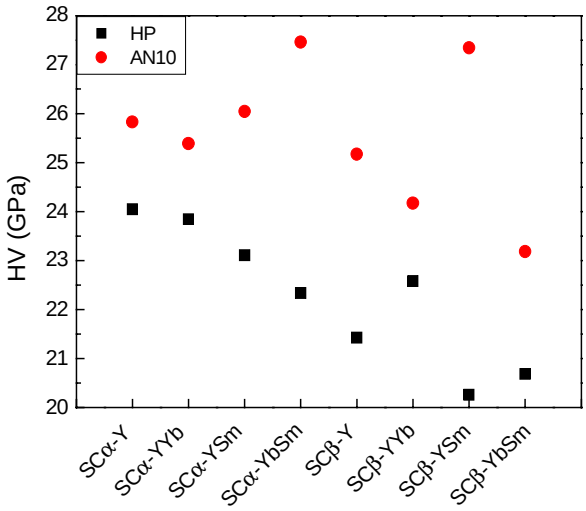

Fig. 3. Vickers macro-hardness of annealed SiC samples measured at 9.81 N load.

that the microstructure and grain boundary phase composition of tested samples are different. Surprisingly, these differences have no significant influence on the nano-hardness of LPS SiC.

The sintered SiC samples contained mainly 3C, 4H, and 6H polytypes. The hardness of single crystal SiC partly depends on the polytype and crystal plane orientation, e.g. the Knoop hardness measured at 100 g load can vary from 2525 kg/mm^2 (3C, plane 100) up to 2954 kg/mm^2 (6H, plane 0001).[14] Such a wide variation of SiC hardness makes even more difficult to evaluate the influence of individual rare-earth oxides in the observed scatter of data, ±2 GPa (Fig. 5).

The nano-hardness values shown in Fig. 5 include information about the hardness of cores, rims; and grain boundary phases. Although we tried so separate the measured values, it was impossible to measure correctly the hardness of grain boundaries by the nano-hardness testing method, because the thickness of grain boundaries is only 1–3 nm, while the edge of the triangular imprints is ∼50 nm. In this case the grain boundary hardness includes information about the hardness of glassy thin film, interface and partially also the hardness of SiC grains. Very few indentations have been found directly in the triple pockets and due to the low statistical value these were not evaluated separately. Some of the grain boundary indentations are shown in Fig. 6. The size of grain boundary imprints is larger in comparison with grain imprints, which indicates that the SiC grains are harder than the grain boundaries, $H_g > H_{gb}$. This observation is plotted

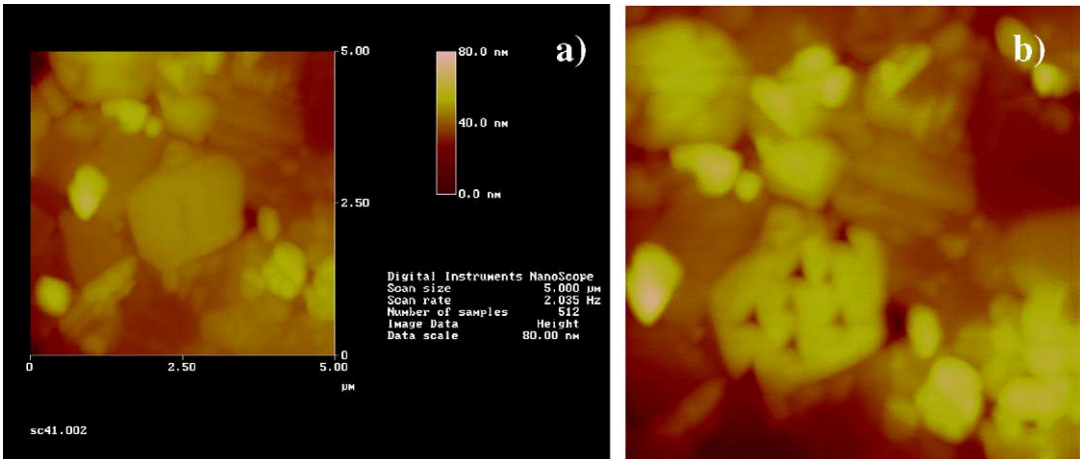

Fig. 4. AFM image of SCα-YbSm sample annealed for 10 h: (a) before indentation and (b) after indentation.

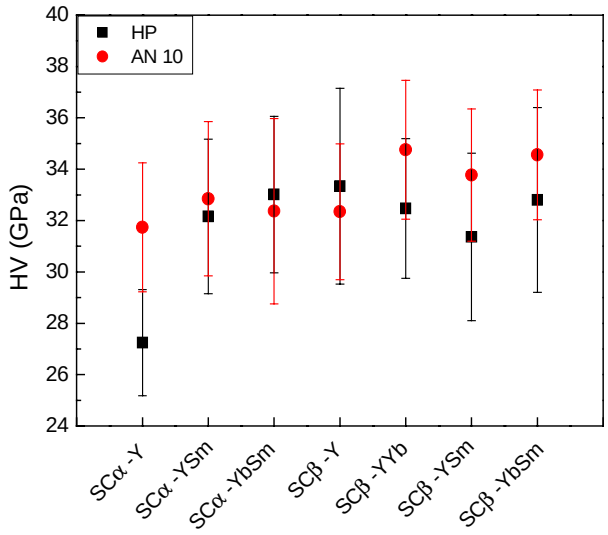

Fig. 5. Nano-hardness of liquid phase sintered SiC.

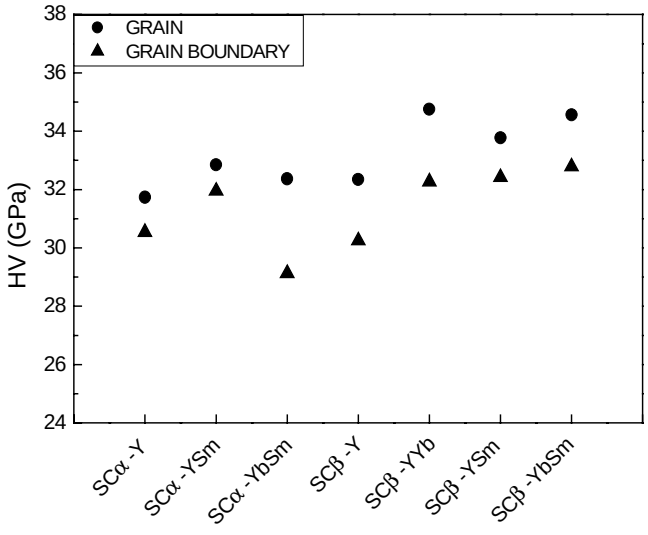

Fig. 7. Nano-hardness of SiC grains and the grain boundaries (GB) after 10 h annealing.

in Fig. 7. The general trend $H_g > H_{gb}$ can be taken only into account, not the absolute values of grain boundary hardness. A certain part of the "grain boundary imprint" is also in the SiC grain, rising the value of H_{gb}. On the other hand, the nanohardness values of SiC grains are influences by the grain boundaries. It was shown that in the case of SiC the diameter of the plastically deformed zone beneath the indent is about five times the lateral width of the observed permanent indent.[15] In our case many of the nano-indents are located close enough to the nearest boundary and incorporate the interface effects. Due to these effects the real value of H_g and H_{gb} should be slightly higher resp. lower, compared with the data shown in Fig. 5.

As it was mentioned above, all samples had a core–rim structure and an example is shown in Fig. 8a. Different properties can be expected owing to the different chemistry of the core and rim. The elemental composition of the core–rim structure of all samples was investigated by EDX analysis. The core consists of Si and C (Fig. 8b), while the rim contains also a small amount of aluminium. There exist a solid solution between SiC and AlN, which caused the incorporation of aluminium into the rim during the dissolution-reprecipitation process. The formation of SiC–AlN solid solution affects the properties of sintered SiC, namely decreases the hardness. The lower micro-hardness of SiC grains in the presence of Al is in agreement with the results of Ruh and Zangvil.[16] These authors described that the micro-hardness values decreased linearly in the SiC–AlN solid solution region with increasing AlN content. Similarly, Sigl and Kleebe reported that in the case of liquid phase sintered SiC using Y_2O_3 sintering additives Y was incorporated into the shell.[13] This effect was not observed in the present study.

Although only a few indents were possible to realize into one grain at 3.5 mN load (Fig. 4), the obtained data give in-

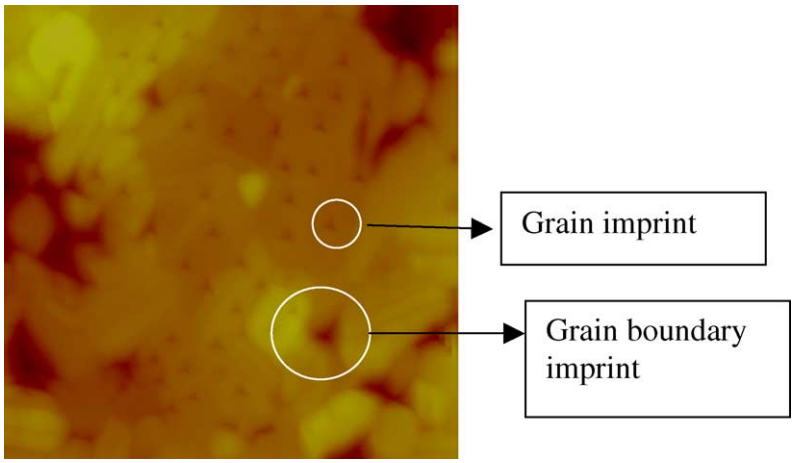

Fig. 6. AFM image of sample SCβ-Y after 10 h annealing.

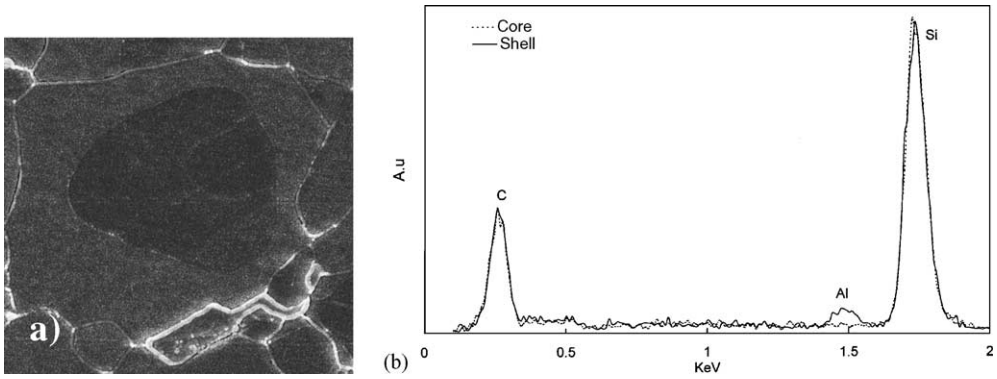

Fig. 8. (a) SEM micrograph of the core–rim structure and (b) EDS analysis of sample SCα-Y.

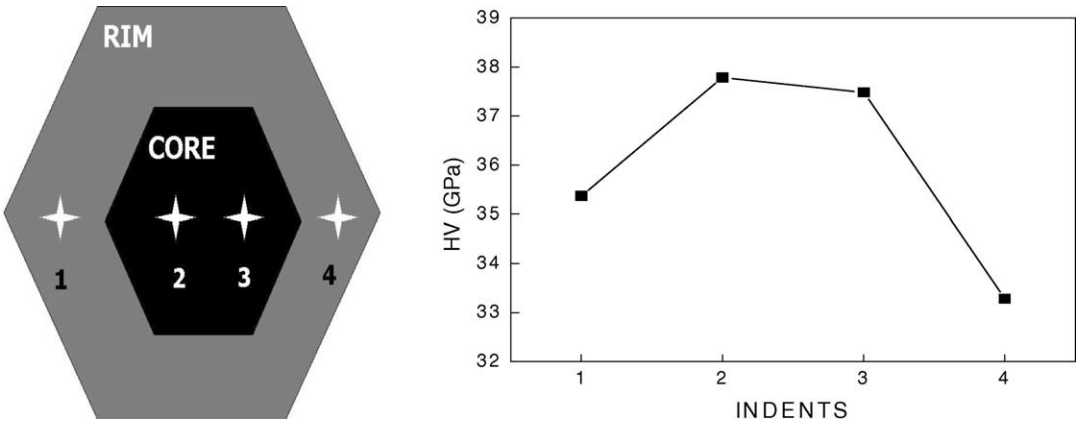

Fig. 9. Nano-indentation of sample SCα-YbSm (across the grain) annealed for 10 h.

formation about the hardness in different positions within one grain. In all cases the central part of grain was harder than the residual part of grain. It can be concluded that using RE_2O_3 + AlN additive system, the core of the grains is harder compared to the rim (Fig. 9). On the other hand, the amount of grain boundary phase decreased owing to the formation of SiC–AlN solid solution, and its composition was shifted towards the pure Re_2O_3. The lower amount of grain boundary phase and its modified chemical composition can improve the high temperature mechanical properties of the liquid phase sintered SiC, which are under investigation.

The high nano-hardness (≅33 GPa) obtained in present study is related to the individual grains. These values can be considered as the mean nano-hardness of SiC and $(SiC–AlN)_{ss}$ single crystals, which the individual core–rim structured grains consist of. Comparable high (25–31 GPa), but macro-hardness values were obtained for the nano-sized SiC sintered with B, B_4C, and C additives.[17] Although, due to the absence of oxide additives in this case the interface bonding has more covalent character and cannot be directly compared with LPS SiC characterized in this work, this microstructure manipulation seems to be a potential for the further development of SiC ceramics materials. Similar result was already reported for the nano-sized polycrystalline Al_2O_3, showing even higher macro-hardness than Al_2O_3 single crystals.[18]

4. Conclusions

Silicon carbide was densified by liquid phase sintering, using rare-earth oxides (Y_2O_3, Yb_2O_3, Sm_2O_3) and AlN as sintering additives. The microstructural analysis of annealed samples at 1850 °C for 10 h showed that SiC grains growth by solution-precipitation mechanism. The SiC grains exhibit the core–rim structure. The core consists of Si and C, however, the rim contains Si, C and contrary to the core also small amount of aluminium. AlN was incorporated into the rim by the formation of solid solution with SiC and consequently decreased the hardness. Decrease of AlN content in the transient liquid phase by forming SiC–AlN solid solution changed the grain boundary chemistry and decreased the amount of liquid phase. The nano-hardness measurements showed that the values depend on the indent position within the individual grain. The hardness of core is significantly higher compared to the hardness of rim which consist of SiC–AlN solid solution.

Nano- versus macro-hardness measurements showed that generally the nano-hardness is higher than the macro-hardness. The reason for this behavior is the influence of several factors like grain boundary phase composition, triple pockets, porosity, grain size, indentation size effect, etc., in polycrystalline materials. Consequently, all these factors have effect on decreasing of the macro-hardness of polycrystalline SiC-based ceramics containing micro-meter sized grains.

Acknowledgements

Financial support of Grants 2003 SO 51/03R 06 00/03R 06 03, VEGA 4072, CE NANOSMART is gratefully acknowledged.

References

1. Prochazka, S., The role of boron and carbon in the sintering of silicon carbide. In *Special Ceramics, Vol 6*, ed. P. Popper. The British Ceramic Research Association, Stoke-on-Trent, UK, 1975, pp. 171–181.
2. Negita, K., Effective sintering aids for silicon carbide ceramics: reactivities of silicon carbide with various additives. *J. Am. Ceram. Soc.* 1986, **69**(12), C308–C310.
3. Sciti, D., Guicciardi, S. and Bellosi, A., Effect of annealing treatment on microstructure and mechanical properties of liquid-phase-sintered silicon carbide. *J. Eur. Ceram. Soc.* 2001, **21**, 621–632.
4. Cheong, D. I., Kim, J. and Kang, S.-J., Effect of isothermal annealing on the microstructure and mechanical properties of SiC ceramics hot-pressed with Y_2O_3 and Al_2O_3 additions. *J. Eur. Ceram. Soc.* 2002, **22**, 1321–1327.
5. Sciti, D. and Bellosi, A., Effects of additives on densification. *J. Mater. Sci.* 2000, **35**, 3849–3855.
6. Rixecker, C., Wiedmann, I., Rosinus, A. and Aldinger, F., High-temperature effect in the fracture mechanical behaviour of silicon carbide liquid-phase sintered with AlN-Y_2O_3 additives. *J. Eur. Ceram. Soc.* 2001, **21**, 1013–1019.
7. Lee, R. R. and Wei, W.-Ch., Fabrication, microstructure, and properties of SiC–AlN ceramic alloys. *Ceram. Eng. Sci. Proc.* 1990, **11**(7/8), 1094–1121.
8. Choi, H.-J., Lee, J.-G. and Kim, Y.-W., Oxidation behavior of liquid-phase sintered silicon carbide with aluminium nitride and rare-earth oxides (Re_2O_3, where Re = Y, Er, Yb). *J. Am. Ceram. Soc.* 2002, **85**(9), 2281–2286.
9. Zhou, Y., Hirao, K., Yamauchi, Y. and Kanzaki, S., Tailoring the mechanical properties of silicon carbide ceramics by modification of the intergranular phase chemistry and microstructure. *J. Eur. Ceram. Soc.* 2002, **22**, 2689–2696.
10. Zhou, Y., Hirao, K., Toriyama, M., Yamauchi, Y. and Kanzaki, S., Effects of intergranular phase chemistry on the microstructure and mechanical properties of silicon carbide ceramics densified with rare-earth oxide and alumina additions. *J. Am. Ceram. Soc.* 2001, **84**(7), 1642–1644.
11. Balog, M., Šajgalík, P., Lenčéš, Z. and Monteverde, F., Influence of α and β SiC seeds on microstructural development and mechanical properties of liquid phase sintered SiC with RE_2O_3 and AlN additives. *Solid State Phenom.* 2003, **90/91**, 273–279.
12. Balog, M., Šajgalík, P., Lenčéš, Z., Kečkéš, J. and Huang, J.-T., Liquid phase sintering of SiC with AlN and rare-earth oxide additives. In *Silicon-based Structural Ceramics for the New Millennium*, ed. M. E. Brito, H.-T. Lin and K. Plucknett. *Ceram. Trans.* 2003, **142**, 191–202.
13. Sigl, L. S. and Kleebe, H.-J., Core/rim structure of liquid-phase-sintered silicon carbide. *J. Am. Ceram. Soc.* 1993, **76**(3), 773–776.
14. Schneider, S. J., *Engineered Materials Handbook, Vol 4*. ASM International, USA, 1987, p. 808.
15. Lankford, J. and Davidson, D. L., Indentation plasticity and microfracture in silicon carbide. *J. Mater. Sci.* 1979, **14**(7), 1669–1675.
16. Ruh, R. and Zangvil, A., Composition and properties of hot-pressed SiC–AlN solid solutions. *J. Am. Ceram. Soc.* 1982, **65**(5), 260–265.
17. Vassen, R. and Stover, D., Processing and properties of nanograin silicon carbide. *J. Am. Ceram. Soc.* 1999, **82**(10), 2585–2593.
18. Krell, A. and Schädlich, S., Nanoindentation hardness of submicrometer alumina ceramics. *Mater. Sci. Eng.* 2001, **A307**, 172–181.